- R E S E A R C H   P A P E R -

The influence of fiber-reinforced shotcrete on the ground settlement in tunnel excavation: a case study of Tabriz metro line 2

Erfan Khoshzaher [a], Shahla Miri Darmarani [a], Hamid Chakeri [a, *], Mohammad Darbor [a] and Hamed Haghkish [b]

[a] Department of Mining Engineering, Sahand University of Technology, Tabriz, Iran.
[b] Department of Civil Engineering, Islamic Azad university, Tabriz, Iran.

ABSTRACT

In recent years, as cities expand and populations increase, the importance of public transportation, particularly subways, and underground spaces, has grown. In-situ concreting in underground areas is time-consuming, costly, and requires significant space for molding. However, shotcrete can be applied quickly with high quality and minimal space needed. The main purpose of this study is to investigate the settlement of the ground surface resulting from tunnel excavation using 3D numerical modelling. This study investigated the use of shotcrete reinforced with recycled and industrial fibers as an alternative tunnel support system in section 4 of the third phase of Tabriz metro line 2. The evaluation of the load-carrying capacity of shotcrete-lattice and fiber-reinforced shotcrete support systems showed that the maximum tensile stress for the preferred support systems is 165.1 MPa and 1.284 MPa, respectively. The results of finite element analysis revealed that shotcrete with 40 kg/m³ of industrial steel fibers and 30 kg/m³ of recycled materials can be a viable alternative to the traditional shotcrete-lattice tunnel support system in Tabriz metro line 2 in terms of resistance and surface settlement properties. The use of recycled fibers is cost-effective, and a smaller quantity of recycled fibers can provide similar mechanical properties compared to a larger quantity of industrial fibers.

Keywords: Numerical modelling, Recycled fibers, Settlement, Shotcrete, Tunnel.

1. Introduction

The increase in city traffic due to population growth causes significant transportation problems. Solving this issue requires the construction of underground transportation systems such as the metro. Although this transportation system has many benefits, building tunnels, especially with low-quality materials, could potentially harm nearby structures by creating stress and ground deformation, that is why it is important to carefully check the stability, ground deformation, and use of strong supports when designing and building a tunnel. Therefore, in tunnel projects, it is necessary to evaluate the settlements and their geology effects on the existing structures [1, 2, 3].

Shotcrete and concrete are some of the most widely used tunnel support systems during the construction of underground excavations and tunnels, and they provide a suitable level of safety and reliability [1, 2]. Shotcrete strengthens the deformed soil layer by enhancing its load-carrying capacity and increasing its resistance to shearing forces [3]. Despite shotcrete's beneficial properties, the primary weaknesses of shotcrete are its low tensile strength and susceptibility to cracking under various loads on coated surfaces. The disadvantages of shotcrete can be reduced by mixing fibers. Adding fibers improves the low tensile strength, low deformation rate, low ductility after cracking, low toughness, and low tensile and bending resistance of concrete structures [4]. The mechanical performance of the composition containing fibers is largely influenced by the properties of the fibers such as the type of fibers, length, diameter, stiffness, strength, and percentage of their use [1, 5, 6].

In general, the design of underground tunnels mainly relies on experimental methods, which largely depend on the previous work experience of the engineering team. On the other hand, analytical techniques, to predict the deformation of rock masses and determine the most suitable support system for them, have been developed [7]. With the advancement of tunnel excavation techniques, the role of numerical simulations has significantly increased in importance. These simulations have become indispensable tools in the design and construction of tunnels, allowing engineers to predict and analyze various factors such as ground stability, structural integrity, and potential risks. By leveraging these advanced computational methods, engineers can optimize tunnel designs, enhance safety measures, and ensure more efficient and cost-effective construction processes [2, 8, 9]. In the context of tunnel support systems, distinct constitutive models can be employed for rock masses and shotcrete based on numerical models using the Finite Element Method (FEM).

Neuner et al. investigated the necessity of 3D numerical modelling for tunnels with high depth and overburden [12]. Chortis et al. and Weifner et al. showed that for NATM and mechanized excavation methods, 3D numerical modelling provides a suitable tool for studying the interaction between tunnels and adjacent structures [13, 14]. Vitali et al. and Gamnitzer et al. showed that 3D numerical modelling of tunnel excavation with the NATM method provides the possibility to investigate the effect of different excavation sequences and allows consideration of the effect of moment and steel arches. In addition, 3D

numerical models are also suitable for the 3D investigation of stresses and deformations of rock masses and shotcrete [15, 16].

De la Fuente, Olander, Massone, Larive, Sheikh, and Monteiro investigated the effect of fibers in shotcrete on the reinforcement of the tunnel support system [3, 17, 18, 19, 20, 21]. Chiai et al. used the finite element model and showed that the presence of fibers in the tunnel support system has advantages such as preventing the formation of cracks and controlling the crack width [22]. Sharghi et al. investigated the performance of recycled steel fibers added to concrete using laboratory tests and numerical modelling. The results indicated that recycled steel fibers are suitable for use as reinforcement. [23]. Majumder et al. obtained a new numerical model for the analysis of excavation in compacted soils using finite element numerical modelling in jointed rock masses [24]. While creating an elastoplastic finite element model with Abaqus software, research was conducted by Congro et al. on how the addition of steel fibers could strengthen tunnel support systems. The study involved analyzing radial displacement and stress distribution around the tunnel. The results demonstrated good alignment between the numerical model and the analytical solution for tunnel excavation [7]. Sharghi et al. investigated the impact of recycled fibers on tunnel segment lining structural integrity in their study. The findings revealed that defects not only widened cracks by five times but also led to the formation of new secondary cracks. Moreover, the results demonstrated that recycled fibers effectively minimized crack expansion and propagation. This research highlights the potential benefits of incorporating recycled materials in tunnel construction for both cost-effectiveness and environmental sustainability [25]. Chakeri et al. conducted a study to investigate the mechanical properties of concrete parts using three types of steel fibers in Tabriz metro line 2 project. The results of various tests showed that the mechanical properties of prefabricated concrete parts are improved by adding fibers [26].

The present study aims to investigate the 3D numerical settlement of the ground surface caused by tunnel excavation. In this study, the impact of using shotcrete reinforced with recycled and industrial fibers as an alternative support system was investigated. The study is applied to a specific and current case, Tabriz metro line 2 offering insights that are directly relevant to ongoing infrastructure projects, whereas many prior studies may have focused on more generalized or theoretical applications. It compares the effectiveness of fiber-reinforced shotcrete with traditional shotcrete-lattice systems, providing a quantitative analysis of their tensile stress capabilities, which adds a new dimension to existing studies. The properties of shotcrete with industrial, recycled fibers, and shotcrete without fibers, were assessed through laboratory tests on cylindrical and cubic samples at the mechanized excavation lab of Tabriz Sahand University of Technology. Essential data for tunnel design includes information from Tabriz's metro line 2 and excavation using the NATM method.

2. Introduction of Tabriz metro line 2 project

The city of Tabriz, with an area of about 225 to 230 km², is located approximately in the southeast-northwest direction (SE-NW) and is 18 km long. The maximum width of the city of Tabriz from north to south is about 14 km and the height is 1340 m above sea level. Tabriz City Metro has five approved lines, of which only the 1st line from El Goli Square to Shahrak Noor with 18 stations is in operation. Also, Tabriz metro line 2 is under construction and its other lines are being studied. Tabriz metro line 2 project with an approximate length of 22.4 km has 22 underground stations that start from the Qaramelk area in the west of Tabriz after passing Qara-Aghaj streets, Danesh-Sara Square, and Abbasi Street arrive at the Baghmishe. It continues to the east and ends at Tabriz International Exhibition. The length of Tabriz urban train line 2 project is divided into three phases. The first two phases are excavated by two EPB-TBMs (Earth Pressure Balance Tunnel Boring Machine). The third phase will be excavated using traditional cut and cover and NATM (New Austrian Tunneling Method) excavation. Figure 1 shows the route of Tabriz metro line 2 along with the stations on the map of

Tabriz city [28].

In this study, the impact of shotcrete reinforced with recycled and industrial fibers is investigated as an alternative support system in the third phase of Tabriz metro line 2 (excavated section using the NATM method). Also, among the excavated sections, section number 4 has been examined in the range of 20+940-21+277 kilometers (Table 1).

Table 1. The scope of implementation of NATM in the study area.

No	Mileage range (km)	Meterage (m)	Excavation method
1	17+675 to 18+275	600	NATM
2	18+660 to 19+011	351	NATM
3	19+630 to 20+400	770	NATM
4	20+940 to 21+277	337	NATM
5	21+375 to 21+790	415	NATM

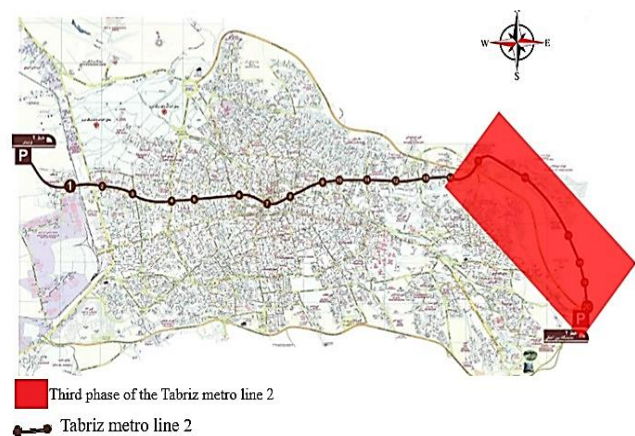Third phase of the Tabriz metro line 2

Tabriz metro line 2

Figure 1. The route and stations of Tabriz metro line 2 [28].

3. Numerical modelling

Most underground structures, such as tunnels, have complex geotechnical, seismic, stability, water flow, temperature and pressure changes. For this reason, numerical methods have been taken into consideration in the design of underground structures. One of the numerical methods for the approximate solution of differential equations is the finite difference method (FDM). In this method, the derivative of functions is approximated by their equivalent differences. To solve the equations, the basis of this method is to use function approximation with Taylor's method. Computational processes of modelling using the finite difference method generally include the construction of model geometry, determination of boundary conditions, behavioral model and material properties, creation of initial balance in the model, application of desired execution conditions, and model solution. One of the most widely used software based on finite difference method is the FLAC software [29].

These days, the finite element method (FEM) is widely utilized due to the growing availability of computational tools and the ability to address complex problems. This approach offers the opportunity to overcome various constraints of analytical and experimental methods, factors such as the geomechanical properties of materials, depth, and stress-strain conditions. The tunnel structure's geometry can influence ground deformation based on the excavation technique. The finite element method views the excavation process as a "step-by-step" procedure. It allows for tracking excavation displacements over time using finite element models. Computational modelling using the finite element method typically involves steps such as defining model geometry, specifying material parameters, creating meshes, and setting boundaries and loading conditions [1, 7, 27]. Abaqus is one of the finite element software tools utilized in this study.

3.1. Properties of support system and excavation method in numerical modelling

Four types of support systems, such as shotcrete and lattice were used in the construction of Tabriz metro line 2. Additionally, three different support systems were examined, incorporating 30 kg/m³ of recycled fibers from tires, as well as 40 kg/m³ and 100 kg/m³ of industrial steel fibers. 2D numerical modelling was conducted using FLAC software to assess the load capacity of support systems, while 3D modelling was performed with Abaqus software to examine ground surface settlement and tunnel wall displacements. The excavation process in the software follows the NATM method and the excavation and construction steps of Tabriz metro line 2. The excavation steps (Figure 2) performed in the software in one excavated step include the following:

1. Excavation of the crown from the upper part of the tunnel.
2. Installation of the support system in the crown section.
3. Excavating the middle part of the upper part.
4. Installation of the tunnel support system in the middle part of the upper part.
5. Excavation of the stairs of the middle part.
6. Excavation of the right wall.
7. Installation of the right wall support system.
8. Excavation of the left wall.
9. Installation of the left wall support system.
10. Excavation of the bottom section.
11. Installation of the floor support system.

3.2. Modelling process using finite difference method and its results

To check the possibility of the load-carrying capacity of support systems, numerical modelling was done using the 2D FLAC software. The properties of section 4 of the third phase of Tabriz metro line 2 are presented in Table 2. After completing the geometry of the model, the Mohr-Columb behavioral model was selected. The parameters used for the soil are described in Table 3 and the properties related to the support system are described in Table 4.

Table 2. Properties of Tabriz metro line 2 tunnel.

Tunnel section	Overburden (m)	Width (m)	Length (m)	Crown radius (m)
horseshoe tunnel	15.5	50	40	5

Excavation in the FLAC software follows the implementation method in Tabriz metro line 2. After each part is excavated, the support system is installed according to the excavated part. Figure 3 shows the model built after balancing and excavation of the tunnel. Also, in Figures 4 to 7, the distribution diagrams of axial force and bending moment in two types of support systems are shown (Table 4).

3.3. Analysis of the load-carrying capacity of the two types of support systems examined in section 4 of the third phase of Tabriz metro line 2.

To analyze the load-carrying capacity of shotcrete-lattice support systems and shotcrete containing steel fibers, the maximum values of axial force and bending moment were determined for both support systems. At first, the analysis of the load-carrying capacity of the shotcrete-lattice support system was performed. The equivalent area (A) and the equivalent moment of inertia (I_X) are as follows:

$$A = 4 \times \left(\frac{\pi(25^2)}{4}\right) = 19.63 \ cm^2 \tag{1}$$

$$I_{X'} = \frac{\pi(12.5^4)}{4} = 1.9175 \ cm^4 \tag{2}$$

Table 3. Soil properties in the numerical model.

Soil	Depth (m)	Density (kg/m³)	Cohesion (Pa)	Friction angle (°)	Young's modulus (MPa)	Poisson's ratio	Bulk Modulus (MPa)	Shear Modulus (MPa)
First Layer	0-1	1680	9806.6	32	30	0.35	32.68	10.89
Second Layer	1-4	1700	10787.3	20	30	0.42	61.29	10.35
Third Layer	4-6	1700	3922.6	31	65	0.34	66.39	23.78
Fourth Layer	6-30	1600	9806.6	22	30	0.39	44.57	10.58
Fifth Layer	30-40	1800	16671.3	24	65	0.37	81.72	23.26

Table 4. Properties of the support system in the numerical model.

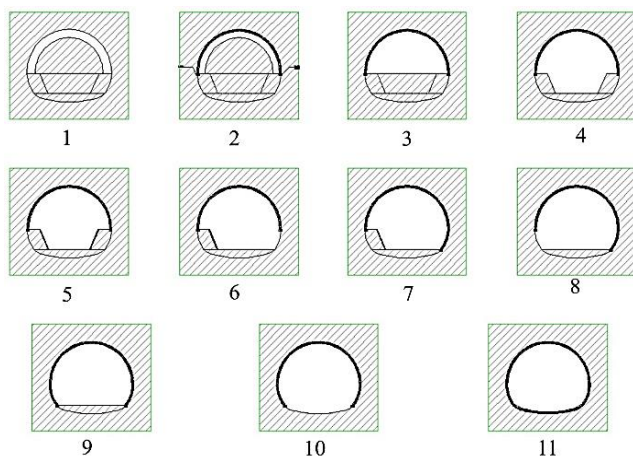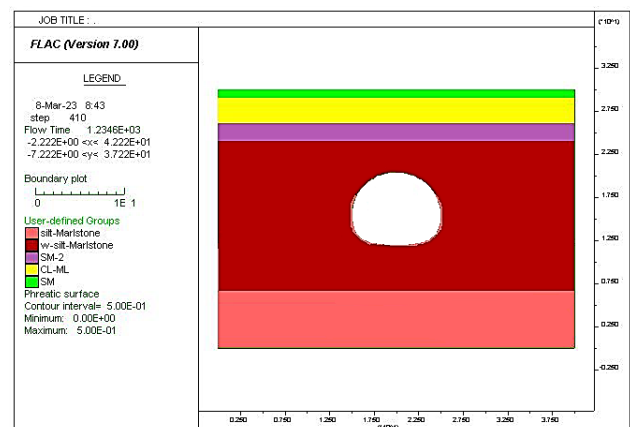| Type of support system	Modulus of elasticity (GPa)	Poisson's ratio	Equivalent area (cm²)	Inertia moment (cm⁴)
Shotcrete + Lattice	200	0.25	19.63	1105.83
Fiber shotcrete	25.5	0.25	30	2256

Figure 2. The excavation steps.

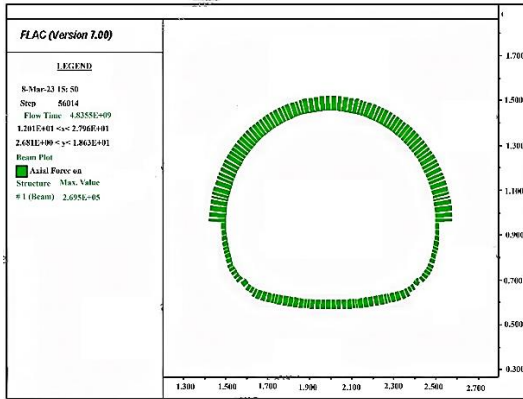**Figure 3.** The position of the layers and excavate the tunnel in the numerical model

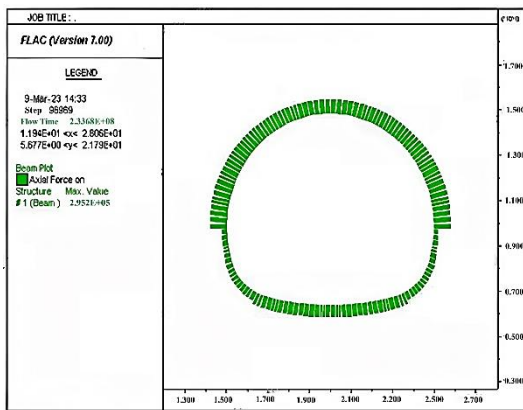**Figure 4.** Axial force distribution diagram in shotcrete and lattice support system (N).

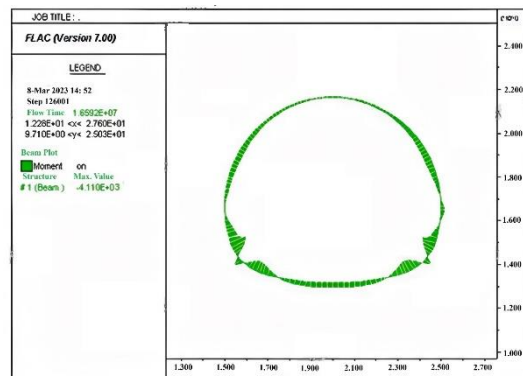**Figure 5.** Axial force distribution diagram in fiber shotcrete support system (N).

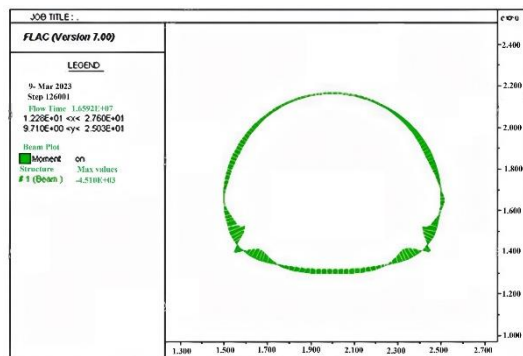**Figure 6.** Bending moment distribution diagram in shotcrete and lattice support system (N.m).

Figure 7. Bending moment distribution chart in fiber shotcrete support system (in N.m)

$$I_X = I_{X'} + Ad^2 = 1.9175 + 19.63 \times 56.25 = 1105.83 \ cm^4 \quad (3)$$

Where:

A is the equivalent area (cm^2), I_X is the equivalent moment of inertia (cm^4), $I_{X'}$ is the moment of inertia around the x axis (cm^4), and d is the distance between axles (cm).

Hence, the area equals 19.63 cm^2, the moment of inertia equals 1105.83 cm^4, the distance from the neutral axis is 75 mm, the maximum axial force is 269.5 kN (as per Figure 3), and the maximum bending moment is -4.1 kN.m (as per Figure 5). These data pertain to the shotcrete-lattice support system. By using the above values in the following relationship, the maximum tensile stress for the desired sections is calculated as follows:

$$\sigma = \frac{P}{A} + \frac{My}{I} = \frac{269.5}{19.63} + \frac{4.1 \times 100 \times 7.5}{1105.83} = 16.51 \ \frac{KN}{cm^2} = 165.10 \ \text{MPa} \quad (4)$$

σ is the maximum tensile strength (MPa), P is the maximum axial force (MPa), A is the equivalent area (cm^2), M is the maximum bending moment, y is the distance from the neutral axis, and I_X is the equivalent moment of inertia (cm^4).

On the other hand, the tensile strength of steel is equal to 400 MPa, and by applying the reliability factor of 1.4, the allowable strength of steel reaches 285.7 MPa. Therefore, the steel frame for tunnel excavation has the necessary stability. To analyze the load-carrying capacity of the shotcrete support system containing steel fibers, the values of the maximum axial force and bending moment were also determined. In this support system, the equivalent area of the frame (A) is 3000 cm^2 (the thickness of the support system is 30 cm and the height of the segment is 1 m), the equivalent moment of inertia (I_X) is 2255000 cm^4, the distance from the neutral axis is 150 mm, the maximum axial force is 295.2 KN (according to Figure 4) and the maximum bending moment is -4.5 kN.m (according to Figure 6). By inputting the above values into the equation below, the maximum tensile stress for the desired sections is determined as follows:

$$\sigma = \frac{P}{A} + \frac{My}{I} = \frac{295.2}{3000} + \frac{4.5 \times 100 \times 15}{225000} = 0.1284 \ \frac{KN}{cm^2} = 1.284 \ \text{Mpa} \quad (5)$$

Where:

σ is the maximum tensile strength (MPa), P is the maximum axial force (MPa), A is the equivalent area (cm^2), M is the maximum bending moment, y is the distance from the neutral axis, and I_X is the equivalent moment of inertia (cm^4).

On the other hand, the tensile strength of fiber shotcrete is equal to 2.69 MPa, which, considering the reliability factor of 1.4, the allowable strength of fiber shotcrete reaches 1.92 MPa. Therefore, fiber shotcrete provides stability for tunnel excavation. Based on numerical modelling in the FLAC software and an analysis of the load-carrying capacity of shotcrete-lattice and shotcrete with steel fibers, the maximum axial force and bending moment values for both support systems are in a safe range. This indicates that the structure is designed to withstand incoming loads effectively.

4. Numerical modelling of section 4 of the third phase of Tabriz metro line 2 using the finite element method

In this section, Abaqus software was used to investigate the settlements resulting from tunnel excavation and compare the results for two types of support systems for section 4 of the third phase of Tabriz metro line 2, including shotcrete + lattice and fiber shotcrete. In the following, numerical modelling with Abaqus is discussed first, and then the results of 3D numerical modelling are presented.

4.1. Geometry and model properties

For all models, the main geometry is solid, homogeneous, and elastoplastic, and the considered behavior model is Mohr-Coulomb. Soil properties and tunnel section information were extracted from Tabriz metro line 2 tunnel project and the length considered for the model is 75 meters by default (Tables 5 and 6). The support system is considered

Table 5. Properties of the numerical model built in the study area.

| Tunnel section	Overburden (m)	Excavation step (m)	High (m)	Width (m)	Length (m)	Crown radius (m)
horseshoe tunnel	15.5	1	40	50	75	5

Table 6. Soil properties in the numerical model in the study area.

Soil	Depth (m)	Density (kg/m³)	Cohesion (Pa)	Friction angle (°)	Young's modulus (MPa)	Poisson's ratio
First Layer	0-1	1680	9806.6	32	30	0.35
Second Layer	1-4	1700	10787.3	20	30	0.42
Third Layer	4-6	1700	3922.6	31	65	0.34
Fourth Layer	6-30	1600	9806.6	22	30	0.39
Fifth Layer	30-40	1800	16671.3	24	65	0.37

elastic for all models. Other properties and excavation steps of the shotcrete support system with lattice follow Tabriz metro line 2 project. The length considered for each part of the support system is proportional to the excavation step and is equal to 1 meter. The properties of fiber shotcrete with industrial and recycled fibers have been extracted through laboratory tests in the Mechanized Excavation Laboratory of Tabriz Sahand University of Technology (Tables 7 and 8). Figure 8 shows the soil geometry and the applied support system by numerical method.

Table 7. Properties of support system geometry in the numerical model in the study area.

Length (m)	Thickness (m)	Excavation step (m)
75	0.3	1
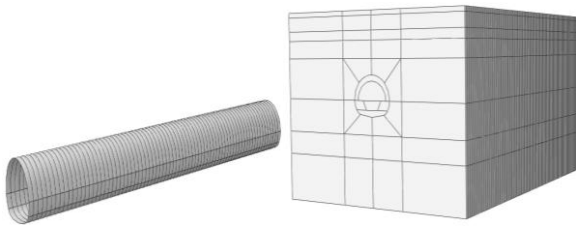
Figure 8. Soil geometry and support system in 3D numerical modelling with finite element method in the study area.

4.2. Meshing and loading conditions

One of the main steps in meshing a model in Abaqus is choosing the shape of the element and the mesh creation technique. The color assigned to each part determines which techniques can be used in meshing that part. In Figure 9, the soil meshing and support system can be seen in section 4 of the third phase of Tabriz metro line 2, which was done with structured and sweep meshing techniques. The approximate size of the elements is from 0.1 to 1m.

For loading, the building load per floor is 1 ton/m² and for vehicles, 2 ton/m² is considered. In this study, a five-story building located above the tunnel is considered based on the tunnel's location, and the traffic load is also factored in. Earth's gravitational force is also applied to the model.

4.3. Discussion and analysis of results

The ground-level settlement was determined by analyzing the vertical displacement of the ground surface and the horizontal displacement of the walls in section 4 of the third phase of Tabriz metro line 2. This analysis was conducted using 3D numerical modelling under conditions where traffic load and building load were applied to the model. In the following, four different types of support systems, including the support system used in Tabriz metro line 2 (shotcrete + lattice) were investigated and the proposed support systems including shotcrete reinforced with industrial and recycled steel fibers were investigated. The analysis of numerical models shows that the vertical displacement of the support system including shotcrete and lattice (Figure 10) is not

much different from the support system of shotcrete containing 40 kg/m³ of industrial fibers and 30 kg/m³ of recycled fibers (Figure 11). In these 3 types of support systems, the maximum displacement of the ground surface in the crown part of the tunnel is equal to 11.25 mm. For shotcrete containing 100 kg/m³ fibers, the maximum amount of vertical movement on the ground surface is in the crown section of the tunnel and is equal to 4.574 mm (Figure 12). This vertical displacement is the lowest amount of displacement in the crown of the tunnel among the investigated support systems. Figure 13 shows the comparison of the vertical displacement of the ground surface in different support systems, considering the traffic load and the load of a 5-story building, in section 4 of the third phase of Tabriz metro line 2. The displacement units in the vertical direction (U) and the wall displacements (U_3) in the profiles are both equal to meters.
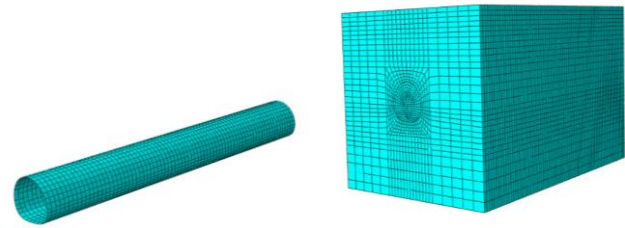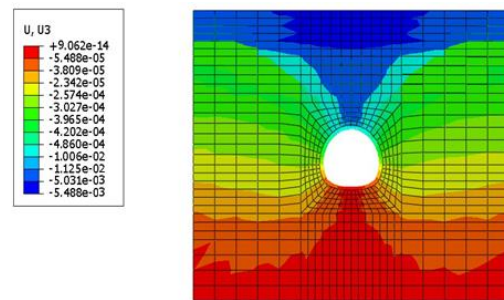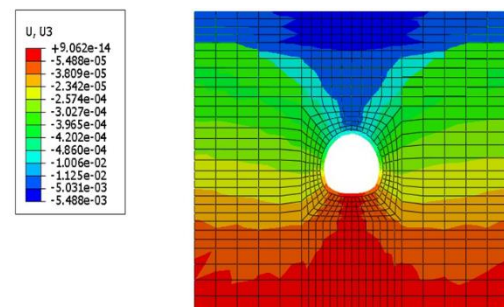

Figure 9. Soil geometry meshing and support system in the study area.

Figure 10. Vertical displacement for a support system, including shotcrete and lattice, considering the traffic load and the load of a 5-story building.

Figure 11. Vertical displacement for fiber shotcrete support systems (SFRS-40) and (SRFS-30) considering the traffic load and the load of a 5-story building.

Table 8. Properties of the support system in the numerical model in the study area.

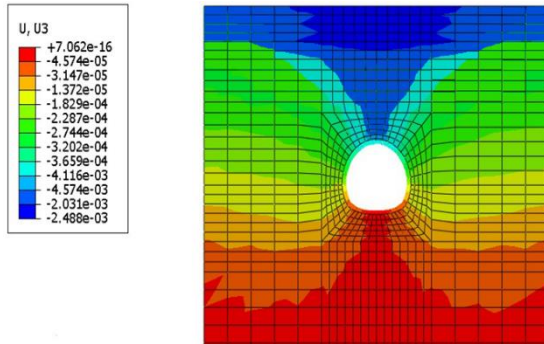| Type of support system	Density (kg/m³)	Modulus of elasticity (GPa)	Poisson's ratio	Thickness (m)
Shotcrete	2170	22.96	0.25	0.3
Shotcrete (ISF-40)	2180	25.5	0.25	0.3
Shotcrete (ISF-30)	2170	26	0.25	0.3
Shotcrete (ISF-100)	2210	29.46	0.25	0.3

Figure 12. Vertical displacement for fiber shotcrete support system (SFRS-100) considering the traffic load and the load of a 5-story building.

Figure 13. Comparing the vertical movement of the ground surface in different support systems considering the traffic load and the load of a 5-story building.
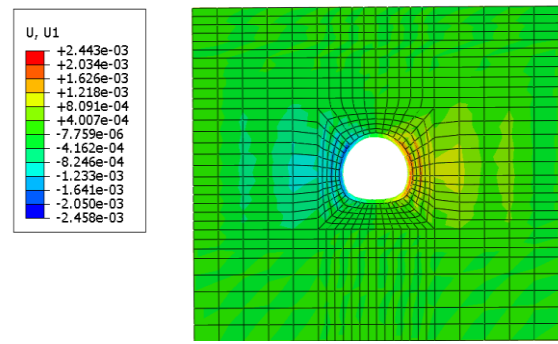

Figure 15. Moving the walls in the x direction for the support system (SFRS-40) and (SFRS-30) considering the traffic load and the load of a 5-story building.
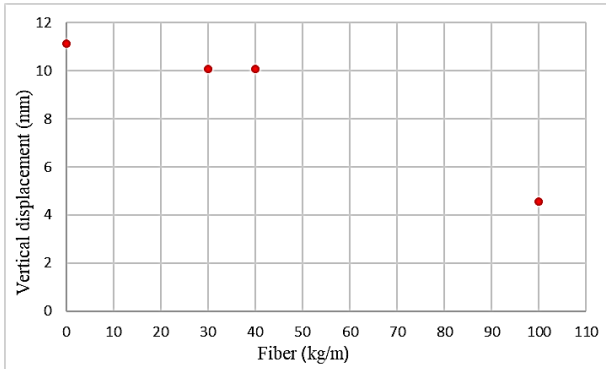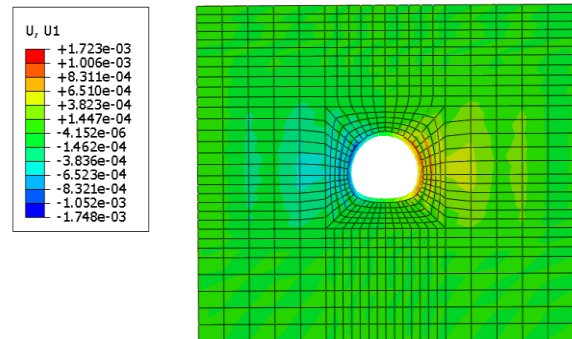

Figure 16. Displacement of walls in x direction for support system (SFRS-100) considering traffic load and load of a 5-story building.

Figure 17. Comparison of the horizontal movement of walls in different support systems considering the traffic load and the load of a 5-story building.

Also, the analysis of the numerical models shows that the displacement of the walls in the x direction in the case where the amounts of industrial and recycled fibers are equal to 40 kg/m³ and 30 kg/m³, respectively, is not much different from the case where the lattice and shotcrete are used as a support system (Figures 14-16). The best condition for moving the walls in the x direction is when the shotcrete contains 100 kg/m³ fibers (Figure 16). Figure 17 shows the comparison of the horizontal movement of the walls in different support systems considering the traffic load and the load of a 5-story building in section 4 of the third phase of Tabriz metro line 2.
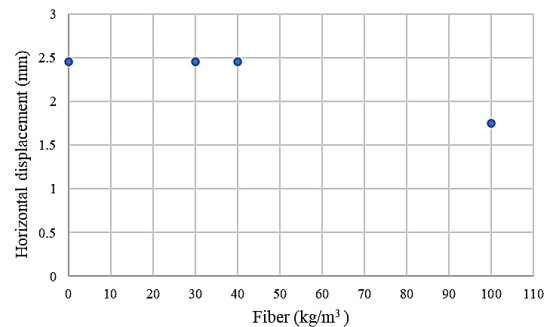
5. Conclusion

Today, the use of steel fiber shotcrete as an alternative to the lattice and shotcrete support system in tunnels is widespread. Compared to the lattice and shotcrete support system, this method solves many of the problems and limitations that exist in the lattice and shotcrete support system. The advantages of this support system include increasing execution speed, reducing costs, increasing resistance, greater flexibility, and reducing volume. Since the installation of the support system, including shotcrete and lattice is time-consuming and difficult and has a high cost in the maintenance department, in this study, the effect of shotcrete reinforced with recycled and industrial fibers was investigated
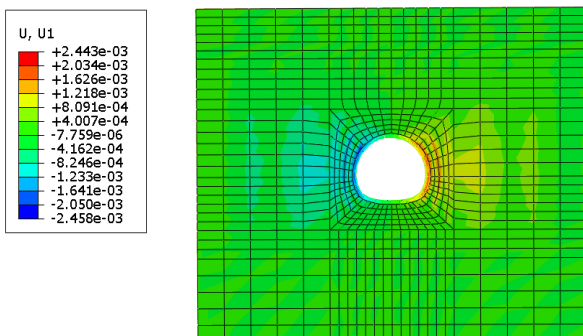

Figure 14. Moving the walls in the x direction for the shotcrete and lattice support system, considering the traffic load and the load of a 5-story building.

as an alternative support system. The results obtained from numerical analyses with the finite difference and finite element methods, considering the traffic load and the load of a 5-story building on the ground in section 4 of the third phase of Tabriz metro line 2 are as follows:

1- The analysis of the load-carrying capacity of the shotcrete-lattice support system showed that the frame equivalent area is 19.63 cm^2, the moment of inertia is 1105.83 cm^4, the maximum axial force is 269.5 kN and the maximum bending moment is -4.1 kN.m. Therefore, the maximum tensile stress for the desired sections is 165.1 MPa. According to the tensile strength of steel and taking into account the reliability factor of 1.4, the allowable strength of steel is 285.7 MPa. Therefore, the steel frame for tunnel excavation has the necessary stability.

2- The analysis of the load-carrying capacity of the fiber shotcrete support system showed that the frame area is 30 cm^2, the inertia is 2256 cm^4, the maximum axial force is 295.2 kN, the maximum bending moment is -4.5 kN.m. Therefore, the maximum tensile stress for the desired sections is 1.284 MPa. According to the tensile strength of fiber shotcrete and considering the reliability factor of 1.4, the permissible strength of fiber shotcrete is 1.92 MPa. Therefore, fiber shotcrete for tunnel excavation has stability.

3- The maximum amount of vertical displacement on the ground level for the support system implemented in Tabriz metro line 2 (shotcrete and lattice) is equal to 11.25 mm. Also, the maximum vertical displacement of the ground surface for the proposed support system that includes shotcrete containing 40 kg/m^3 of industrial steel fibers or shotcrete containing 30 kg/m^3 of recycled fibers is equal to 11.25 mm for both support systems. In addition, the maximum vertical displacement of the ground surface for the shotcrete support system containing 100 kg/m^3 of industrial steel fibers is equal to 4.574 mm.

4- The maximum horizontal displacement in the tunnel walls for the support system implemented in Tabriz metro line 2 (shotcrete and lattice) is equal to 2.458 mm. Also, the maximum horizontal displacement of the walls for the proposed support system, including shotcrete containing 40 kg/m^3 of industrial steel fibers or shotcrete containing 30 kg/m^3 of recycled fibers for both support systems is equal to 2.458 mm. In addition, the maximum horizontal displacement of the walls for shotcrete containing 100 kg/m^3 of industrial steel fibers are equal to 1.748 mm.

5- The obtained results showed that in terms of load-carrying capacity and settlement, shotcrete with 2% steel fibers (40 kg/m^3) and 1.5% recycled fibers (30 kg/m^3) can be a suitable alternative for the support system of Tabriz metro line 2, including latis and shotcrete. On the other hand, the use of recycled fibers from tires is very economical in terms of mechanical properties, a smaller amount of recycled fibers can replace a larger amount of industrial steel fibers.

References

[1] Ağbay, E., & Topal, T. (2020). Evaluation of twin tunnel-induced surface ground deformation by empirical and numerical analyses (NATM part of Eurasia tunnel, Turkey). Computers and Geotechnics, 119, 103367. doi:https://doi.org/10.1016/j.compgeo.2019.103367

[2] Khan, M. U., Tahir, M. U., Emad, M. Z., Raza, M. A., & Saki, S. A. (2023). Investigating strength anisotropy of plain and steel fiber reinforced shotcrete. Mining, Metallurgy & Exploration, 40(1), 291-303.doi: https://doi.org/10.1007/s42461-022-00715-9

[3] De la Fuente, A., Pujadas, P., Blanco, A., & Aguado, A. (2012). Experiences in Barcelona with the use of fibres in segmental linings. Tunnelling and Underground Space Technology, 27(1), 60-71.doi: https://doi.org/10.1016/j.tust.2011.07.001

[4] Balagopal, V., Panicker, A. S., Arathy, M. S., Sandeep, S., & Pillai, S. K. (2022). Influence of fibers on the mechanical properties of cementitious composites-a review. Materials Today: Proceedings, 65, 1846-1850. doi: https://doi.org/10.1016/j.matpr.2022.05.023

[5] Choumanidis, D., Badogiannis, E., Nomikos, P., & Sofianos, A. (2016). The effect of different fibres on the flexural behaviour of concrete exposed to normal and elevated temperatures. Construction and Building Materials, 129, 266-277. doi: https://doi.org/10.1016/j.conbuildmat.2016.10.089

[6] Wu, Z., Shi, C., He, W., & Wu, L. (2016). Effects of steel fiber content and shape on mechanical properties of ultra high performance concrete. Construction and building materials, 103, 8-14. doi: https://doi.org/10.1016/j.conbuildmat.2015.11.028

[7] Congro, M., de Alencar Monteiro, V. M., de Andrade Silva, F., Roehl, D., & Brandão, A. L. (2023). A novel hybrid model to design fiber-reinforced shotcrete for tunnel linings. Tunnelling and Underground Space Technology, 132, 104881. doi:

https://doi.org/10.1016/j.tust.2022.104881

[8] Naseri, S., & Bahrani, N. (2021). Design of initial shotcrete lining for a mine shaft using two-dimensional finite element models considering excavation advance rate. Geotechnical and Geological Engineering, 39, 4709-4732.doi: https://doi.org/10.1007/s10706-021-01773-4

[9] Neuner, M., Schreter, M., Gamnitzer, P., & Hofstetter, G. (2020). On discrepancies between time-dependent nonlinear 3D and 2D finite element simulations of deep tunnel advance: A numerical study on the Brenner Base Tunnel. Computers and Geotechnics, 119, 103355. doi: https://doi.org/10.1016/j.compgeo.2019.103355

[10] Alejano, L. R., Rodriguez-Dono, A., Alonso, E., & Manín, G. F. (2009). Ground reaction curves for tunnels excavated in different quality rock masses showing several types of post-failure behaviour. Tunnelling and Underground Space Technology, 24(6), 689-705. doi:

https://doi.org/10.1016/j.tust.2009.07.004

[11] Alonso, E., Alejano, L. R., Varas, F., Fdez-Manin, G., & Carranza-Torres, C. (2003). Ground response curves for rock masses exhibiting strain-softening behaviour. International journal for numerical and analytical methods in geomechanics, 27(13), 1153-1185. doi:

https://doi.org/10.1002/nag.315

[12] Neuner, M., Schreter, M., Gamnitzer, P., & Hofstetter, G. (2020). On discrepancies between time-dependent nonlinear 3D and 2D finite element simulations of deep tunnel advance: A numerical study on the Brenner Base Tunnel. Computers and Geotechnics, 119, 103355. doi: https://doi.org/10.1016/j.compgeo.2019.103355

[13] Chortis, F., & Kavvadas, M. (2021). Three-dimensional numerical investigation of the interaction between twin tunnels. Geotechnical and Geological Engineering, 39(8), 5559-5585.doi: https://doi.org/10.1007/s10706-021-01845-5

[14] Weifner, T., & Bergmeister, K. (2020). 3D simulations for the Brenner Base Tunnel considering interaction effects. In Tunnels and Underground Cities: Engineering and Innovation meet Archaeology, Architecture and Art (pp. 3355–3364). CRC Press.

[15] Vitali, O. P., Celestino, T. B., & Bobet, A. (2022). Construction strategies for a NATM tunnel in Sa˜o Paulo, Brazil, in residual soil. Underground Space, 7, 1–18. doi:https://doi.org/10.1016/j.undsp.2021.04.002

[16] Gamnitzer, P., Neuner, M., Schreter-Fleischhacker, M., Dummer, A., Mader, T., Smaniotto, S., & Hofstetter, G. (2024). Key features of numerical models for the FE-simulation of deep tunnel advance by the NATM. Underground Space, 14, 357-376. doi: https://doi.org/10.1016/j.undsp.2023.06.007

[17] Sjölander, A., & Ansell, A. (2017). Numerical simulations of restrained shrinkage cracking in glass fibre reinforced shotcrete slabs. Advances in Civil Engineering, 2017(1), 8987626. doi: https://doi.org/10.1155/2017/8987626

[18] Massone, L. M., & Nazar, F. (2018). Analytical and experimental evaluation of the use of fibers as partial reinforcement in shotcrete for tunnels in Chile. Tunnelling and Underground Space Technology, 77, 13-25. doi: https://doi.org/10.1016/j.tust.2018.03.027

[19] Larive, C., Bouteille, S., Berthoz, N., & Zappelli, S. (2020). Fiber-reinforced sprayed concrete as a permanent tunnel lining. Structural Engineering International, 30(4), 498-505. doi: https://doi.org/10.1080/10168664.2020.1735981

[20] Sheikh, K. A., & Saif, A. (2020). Steel Fibre-Reinforced Shotcrete as an alternative to conventional concrete tunnel lining: A case study of Gulpur Hydropower Project. Geomechanics and Geoengineering, 15(4), 252-262. doi: https://doi.org/10.1080/17486025.2019.1639831

[21] de Alencar Monteiro, V. M., & de Andrade Silva, F. (2021). On the design of the fiber reinforced shotcrete applied as primary rock support in the Cuiabá underground mining excavations: A case study. Case Studies in Construction Materials, 15, e00784. doi: https://doi.org/10.1016/j.cscm.2021.e00784

[22] Chiaia, B., Fantilli, A. P., & Vallini, P. (2009). Combining fiber-reinforced concrete with traditional reinforcement in tunnel linings. Engineering Structures, 31(7), 1600-1606. doi: https://doi.org/10.1016/j.engstruct.2009.02.037

[23] Sharghi, M., Chakeri, H., Afshin, H., Török, Á., & Dias, D. (2021). Investigation of the feasibility of using recycled steel fibers in tunnel lining segments. Tunnelling and Underground Space Technology, 110, 103826. doi: https://doi.org/10.1016/j.tust.2021.103826

[24] Majumder, D., Viladkar, M. N., & Singh, M. (2023). Numerical modelling of tunnels excavated in squeezing ground condition: A case study. Arabian Journal for Science and Engineering, 48(4), 4657-4673. doi: https://doi.org/10.1007/s13369-022-07098-5

[25] Sharghi, M., Afshin, H., Chakeri, H., Dias, D., & Török, Á. (2023). Structural and environmental performance of recycled steel fiber reinforced concrete segment under the thrust force of the tunnel boring machine jacks. Structural Concrete, 24(2), 2638-2661. doi:https://doi.org/10.1002/suco.202200538

[26] Chakeri, H., Darbor, M., Maleki, F., & Minaee, T. (2023). Experimental investigation of steel fibers' effect on the improvement of mechanical properties of concrete segmental lining in mechanized tunneling. Rudarsko-geološko-naftni zbornik, 38(3), 55-63. doi:https://doi.org/10.17794/rgn.2023.3.5

[27] Zhang, Z. X., Liu, C., Huang, X., Kwok, C. Y., & Teng, L. (2016). Three-dimensional finite-element analysis on ground responses during twin-tunnel construction using the URUP method. Tunnelling and Underground Space Technology, 58, 133-146. doi: https://doi.org/10.1016/j.tust.2016.05.001

[28] Tabriz Urban Railway Organization, http://tabrizmetro.ir/?PageID=69

[29] Chapra, S. C., & Canale, R. P. (1988). Numerical Methods for EngineersMcGraw-Hill. Inc., New York.

[1] Backus, G. E., Gilbert, F., (1967). Numerical Applications of a Formalism for Geophysical Inverse Problems. Geophysical Journal of the Royal Astronomical Society, 13, 1-3, 247–276.

[2] Backus, G.E., Gilbert, F., (1968). The Resolving power of Gross Earth Data, Geophysical Journal of the Royal Astronomical Society, 16, 169–205.

[3] Backus, G.E., Gilbert, F., (1970). Uniqueness in the Inversion of inaccurate Gross Earth Data, Philosophical Transactions of the Royal Society of London A, 266, 123-192.

[4] Mosegaard, K., Tarantola, A., (1995). Monte Carlo sampling of solutions to inverse problems. J Geophys Res Solid Earth 100(B7),12431–12447

[5] Gouveia, W. P., Scales, J. A., (1997). Resolution of seismic waveform inversion: Bayes versus Occam, Inverse Problems 13, 323–349.

[6] Moorkamp M, Jones AG, Eaton DW (2007) Joint inversion of teleseismic receiver functions and magnetotelluric data using a genetic algorithm: are seismic velocities and electrical conductivities compatible? Geophysical Research Letters, 34(16):L16, 311

[7] Akca I, Basokur AT (2010) Extraction of structure-based geoelectric models by hybrid genetic algorithms. Geophysics 75(1):F15–F22

[8] Roy L, Sen MK, Blankenship DD, Stoffa PL, Richter TG (2005) Inversion and uncertainty estimation of gravity data using simulated annealing: an application over Lake Vostok, East Antarctica. Geophysics 70(1):J1–J12

[9] Wang R, Yin C, Wang M, Wang G (2012) Simulated annealing for controlled-source audio-frequency magnetotelluric data inversion. Geophysics 77(2):E127–E133.

[10] Reading, A. M., Cracknell, M. J., and Sambridge, M., (2011). Turning geophysical data into geological information or why a broader range of mathematical strategies is needed to better enable discovery. Preview, 151,24–29. https://doi.org/10.1071/PVv2011n151p24.

[11] Fernández-Muñiz , Z., Khaniani, H., and , J. L. (2019). Data kit inversion and uncertainty analysis. Journal of Applied Geophysics, 161, 228–238.

[12] Efron, B., (1979). Bootstrap methods: another look at the jackknife. Ann. Statist. 7, 1-26.

[13] McLaughlin, K.L., (1988). Maximum-likelihood event magnitude estima- tion with bootstrapping for uncertainty estimation, Bull. seism. Soc. Am., 78(2), 855–862.

[14] Tichelaar, B.W. and Ruff, L.J., (1989). How good are our best models? Jack- knifing, bootstrapping, and earthquake depth, EOS, Trans. Am. geophys. Un., 55(12), 1613–1624.

[15] Shearer, P.M., (1997). Improving local earthquake locations using the l1 norm and waveform cross correlation: application to the Whittier Narrows, California, aftershock sequence, Journal of Geophysical Research, 102(B4), 8269–8283.

[16] Parsekian, A. D., and Grombacher, D. (2015). Uncertainty estimates for surface nuclear magnetic resonance water content and relaxation time profiles from bootstrap statistics. Journal of Applied Geophysics, 119, 61–70. https://doi.org/10.1016/j.jappgeo.2015.05.005.

[17] Hertrich, M., (2008). Imaging of groundwater with nuclear magnetic resonance: Progress in Nuclear Magnetic Resonance Spectroscopy, 53, 227–248.

[18] Schnaidt, S., and Heinson, G. (2015). Bootstrap resampling as a tool for uncertainty analysis in 2-D magnetotelluric inversion modelling. Geophysical Journal International, 203(1), 92–106. https://doi.org/10.1093/gji/ggv264.

[19] Campanya, J., Ledo, J., Queralt, P., Marcuello, A. and Jones, A.G., (2014). A new methodology to estimate magnetotelluric (MT) tensor relationships: estimation of local transfer-functions by combining interstation transfer- functions (ELICIT), Geophysical Journal International, 198(1), 484–494.

[20] Neukirch, M. and Garcia, X., 2014. Nonstationary magneto-telluric data processing with instantaneous parameter, Journal of Geophysical Research, 119, 1634–1654.

[21] Ebtehaj, M., Moradkhani, H., and Gupta, H. V. (2010). Improving robust-ness of hydrologic parameter estimation by the use of moving block bootstrap resampling, Water Resources Res., 46, W07515,

[22] Kunsch, H. R. (1989). The jackknife and the bootstrap for general stationary observations. Ann.Statist. 17 1217–1261.

[23] Liu, R. Y. and Singh, K. (1992). Moving blocks jackknife and bootstrap capture weak dependence. In Exploring the Limits of Bootstrap (R. Lepage and L. Billard, eds.) 225–248. Wiley, New York.

[24] Fernández Martínez, J. L., Zulima Fernández Muñiz, M and Tompkins, M. J., (2012). On the topography of the cost functional in linear and nonlinear inverse problems, Geophysics 77: W1-W15.

[25] Constable, S. C., R. L. Parker, and C. G. Constable, (1987). Occam's inversion: A practical algorithm for generating smooth models from electromagnetic sounding data: Geophysics, 52,289–300, doi: 10.1190/1.1442303.

[26] Aster, R., Borchers, B., and Thurber, C. (2005). Parameter estimation and inverse problems. Elsevier.

[27] Ghosh, D.P., (1971). The application of linear filter theory to the direct interpretation of geoelectrical resistivity sounding measurements Geophysical Prospecting, 19, 192-217.

[28] McNeill, J.D., (1980). Electromagnetic Terrain Conductivity Measurement at Low Induction Numbers. Tech note TN-6. Geonics Ltd, Mississauga, ON, Canada.